Available online at www.sciencedirect.com
ScienceDirect
Bioelectrochemistry 69 (2006) 82–87
Bioelectrochemistry
www.elsevier.com/locate/bioelechem

Redox kinetics of adriamycin adsorbed on the surface of graphite and mercury electrodes

Šebojka Komorsky-Lovrić

Center for Marine and Environmental Research "Ruđer Bošković" Institute, P.O. Box 180 10002, Zagreb, Croatia

Received 12 August 2005; received in revised form 13 October 2005; accepted 18 October 2005
Available online 27 January 2006

Abstract

Kinetics of the surface redox reactions of adriamycin (doxorubicin hydrochloride) adsorbed on paraffin-impregnated graphite electrode (PIGE) and on mercury electrode is measured by square-wave voltammetry. In 0.9 mol/L KNO_3 buffered to pH 4.65, the standard electrode reaction rate constants of the first quinone/hydroquinone redox couple (see Scheme 2) on PIGE and mercury are $k_{s1}=49\pm12$ s^{-1} and $k_{s1}=147\pm36$ s^{-1}, respectively. Under the same conditions, the standard rate constant of the second redox couple on the PIGE is smaller than 4 s^{-1} and the electron transfer coefficient of the reduction is $\alpha_2=0.35$.

Keywords: Adriamycin; Doxorubicin; Kinetics; Redox reaction; Surface; Graphite electrode; Mercury electrode; Square-wave voltammetry

1. Introduction

Adriamycin is the commercial name for doxorubicin hydrochloride which consists of naphthacenequinone nucleus linked through a glycosidic bond to an amino sugar, daunosamine (see Scheme 1). Doxorubicin is a cytotoxic anthracycline antibiotic isolated from cultures of *Streptomyces peucetius* var. *caesius* [1]. The molecule is amphoteric, containing acidic functions in the ring phenolic groups and basic function in the sugar amino group. The anthracycline ring is lipophilic, while hydroxyl groups and amino sugar are hydrophilic [2–4]. Adriamycin has been used to produce regression in disseminated neoplastic conditions such as leukemia, neuroblastoma, sarcomas and carcinoma [1,2,5–10]. The cytotoxic effect of doxorubicin on malignant cells and its toxic effects on various organs are thought to be related to the binding of the antibiotic to the cell membranes and plasma proteins and to the intercalation of the planar anthracycline nucleus into the DNA double helix. Intercalation inhibits nucleotide replication and action of DNA and RNA polymerases [11–19].

Adriamycin is electroactive substance. The redox centers are quinone and hydroquinone groups, which are marked as 1. and 2. in Scheme 1 [16–24]. Also, adriamycin is strongly adsorbed to the surface of mercury [16,20], pyrolytic graphite [17], carbon paste [21,22] and glassy carbon electrodes [23]. These phenomena were utilized for electroanalytical purposes [22,23,25–30].

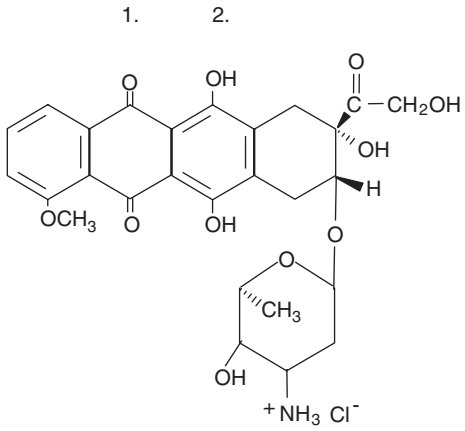

Scheme 1. Structural formula of adriamycin. The numbers mark quinone and hydroquinone redox centers.

E-mail address: slovric@rudjer.irb.hr.

1567-5394/$ - see front matter © 2005 Elsevier B.V. All rights reserved.
doi:10.1016/j.bioelechem.2005.10.006

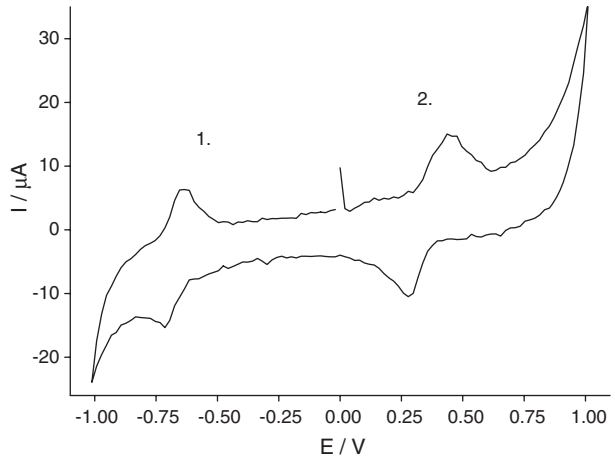

Fig. 1. Staircase cyclic voltammogram of adriamycin adsorbed on the surface of paraffin-impregnated graphite electrode (PIGE) and immersed into 0.9 M KNO_3, pH 4.65. A starting potential is 0 V vs. Ag/AgCl/3 M KCl and a scan rate is 0.1 V/s.

In this article, the electrode reactions of adsorbed adriamycin are analyzed by square-wave voltammetry. The objective is to measure the kinetics of the surface redox reactions by using the method of "quasi-reversible maximum" that was previously applied to the redox kinetics of azobenzene [31], alizarine red S [32] and cinnoline [33].

2. Experimental

Adriamycin (doxorubicin hydrochloride, 2 mg/mL in 0.9% NaCl, pH 3 (HCl) aqueous solution) was obtained from the Cell Pharm GmbH (Hannover, Germany), and used without further purification. KNO_3 and 0.1 mol/L buffer solution pH 4.65 (sodium citrate–HCl) (both Kemika, Zagreb, analytical grade) were used as received. Water was demineralized by ionic exchangers Millipore Milli Q until its specific resistance was 18.2 MΩ cm. Supporting electrolytes were prepared by adding 1 mL of buffer solution to 9 mL of 1 mol/L KNO_3.

The voltammetric measurements were performed with a multimode polarograph Autolab 30 (EcoChemie, Utrecht). The working electrode were a spectral-grade paraffin-impregnated graphite rod (PIGE, diameter 5 mm, length 5 cm) and A Static Mercury Drop Electrode Assembly 303 A (Princeton Applied Research, a drop area 0.015 cm^2). The Pt wire was an auxiliary electrode and Ag/AgCl/3 M KCl (Metrohm) was a reference electrode (E=0.208 V versus SHE).

The experiments with the mercury drop electrode were performed in 1.72×10^{-4} M solution of adriamycin in the supporting electrolyte. Adriamycin was adsorptively accumulated on the mercury surface during 30 s, at −0.1 V, without stirring the solution.

On PIGE, the adsorbed layer of adriamycin was prepared by immersing PIGE into the stock solution of adriamycin for 3 min. Then the electrode was rinsed with water and transferred into the electrochemical cell filled with a pure supporting electrolyte. This method was recommended by Chaney and Baldwin [22] and Oliveira-Brett et al. [23]. They demonstrated its superiority over the accumulation in situ.

3. Results and discussion

A cyclic voltammogram of adriamycin adsorbed on PIGE is shown in Fig. 1. Two pairs of peaks, with medium potentials −0.68 and +0.35 V, can be noticed. According to literature data [16,18–21,23], these correspond to the reduction of quinone (1.) and the oxidation of hydroquinone (2.) centers. These electrode reactions are shown in Scheme 2. For the scan

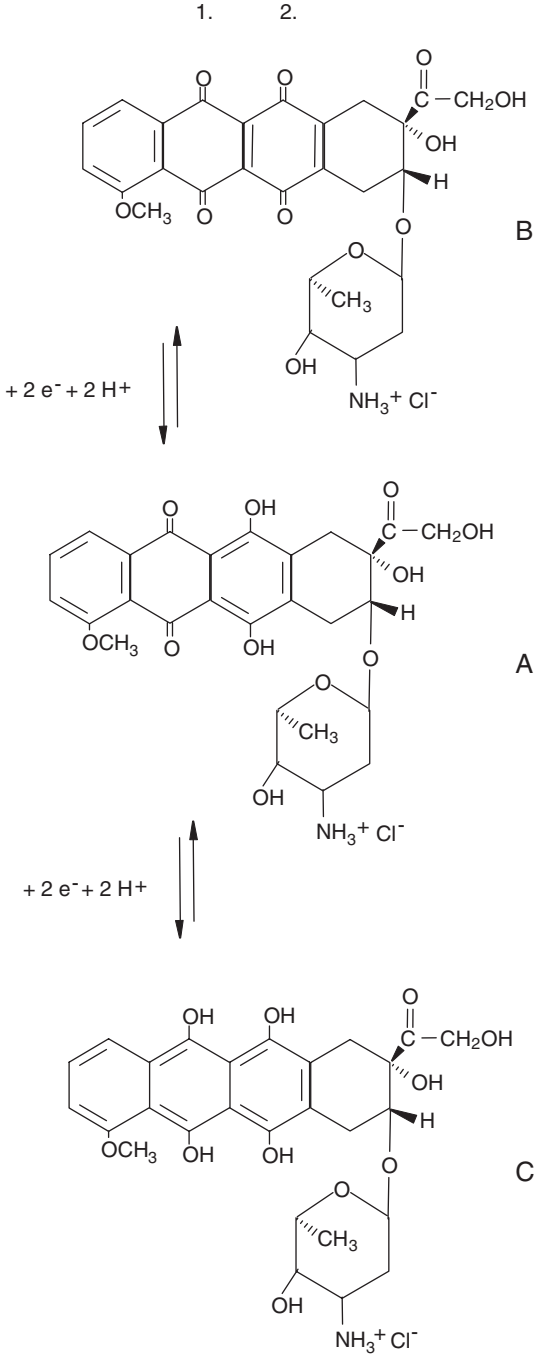

Scheme 2. Electrode reactions of adriamycin (A) and its oxidized (B) and reduced (C) forms.

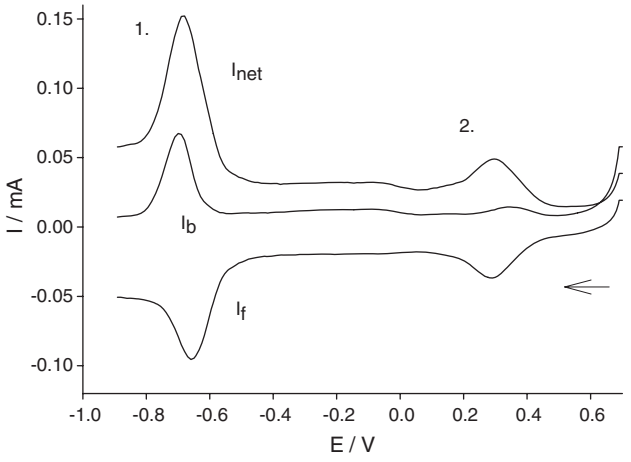

Fig. 2. Square-wave voltammogram of adriamycin adsorbed on the PIGE and immersed into 0.9 M KNO_3, pH 4.65. A net response (I_{net}) and its forward (I_f) and backward (I_b) components. A starting potential is 0.7 V, a frequency is 50 Hz, an amplitude is 50 mV and a potential increment is −2 mV. The numbers 1. and 2. mark the responses of two redox centers.

rate of 0.1 V/s, the peak separations of the first and the second electrode processes are 80 and 160 mV, respectively. At 0.05 V/s, the separations decrease to 60 and 80 mV, respectively. This shows that both electrode processes are kinetically controlled, but the first one is faster than the second one. Considering that there is no dissolved adriamycin in the electrolyte, this result shows that all three redox forms of adriamycin are strongly adsorbed on the electrode surface. The same was observed with carbon paste [22] and glassy carbon electrodes [23].

The responses of these two electrode processes in square-wave voltammetry are shown in Fig. 2. The starting potential is +0.7 V. So, initially, on the electrode surface the adsorbed adriamycin exists in its oxidized form B (see Scheme 2). The forward (reductive) component of response (I_f) corresponds to the reduction of quinone groups, while the backward (oxidative) component (I_b) corresponds to the re-oxidation of hydroquinone groups. The net response is the difference between the two components: $I_{net}=I_b-I_f$. The two peaks of the net response appear at −0.68 and +0.30 V, respectively. The backward component of the first response is much bigger than the one of

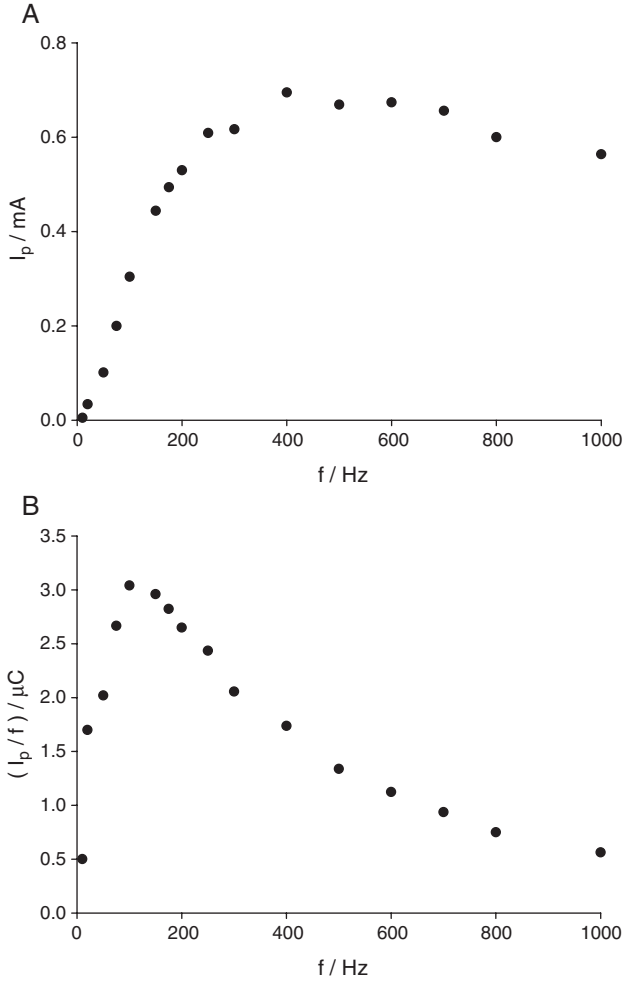

Fig. 3. Square-wave voltammetry of the first redox center of adriamycin adsorbed on PIGE. Dependence of the net peak current (A) and the ratio between the net peak current and frequency (B) on the frequency. Experimental conditions are as in Fig. 2.

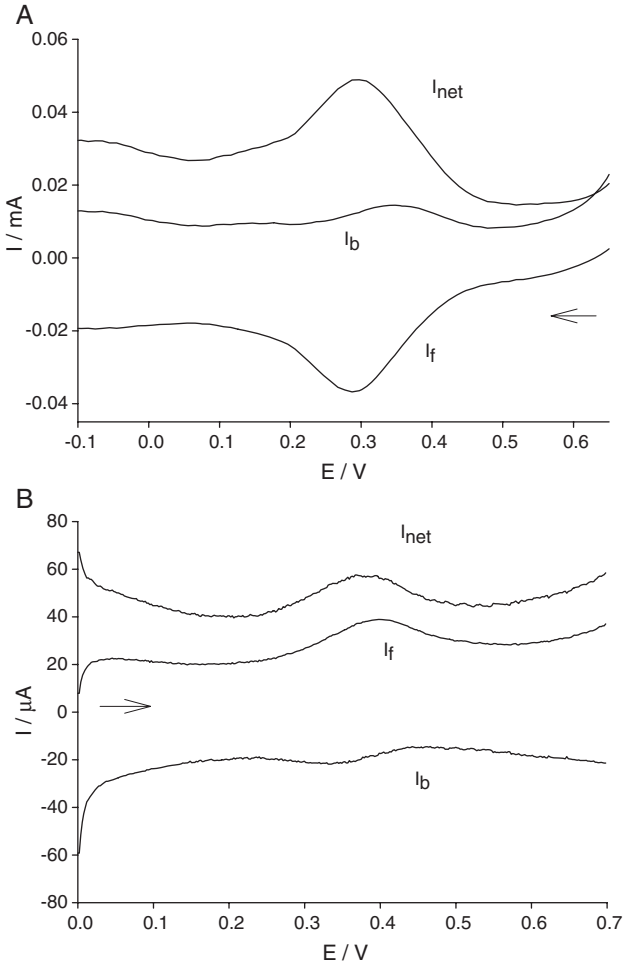

Fig. 4. Adriamycin adsorbed on PIGE and immersed into 0.9 M KNO_3, pH 4.65. Square-wave voltammetry of the second redox center. Dependence of the net response and its components on the starting potential: $E_{st}=0.7$ V (A) and 0 V (B); $E_{sw}=50$ mV, $f=10$ Hz and $dE=-2$ mV (A) and 2 mV (B).

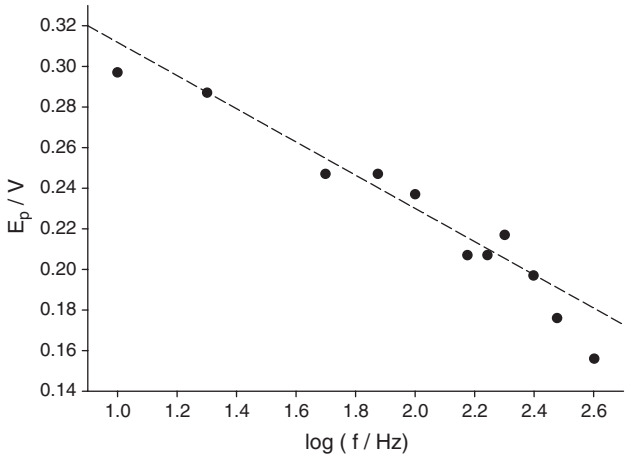

Fig. 5. Dependence of the peak potential of the second net response of adriamycin adsorbed on PIGE on the logarithm of square-wave frequency. Experimental conditions are as in Fig. 2.

the second response. This means that the first electrode reaction is much faster than the second one, in agreement with the results obtained by using a staircase cyclic voltammetry.

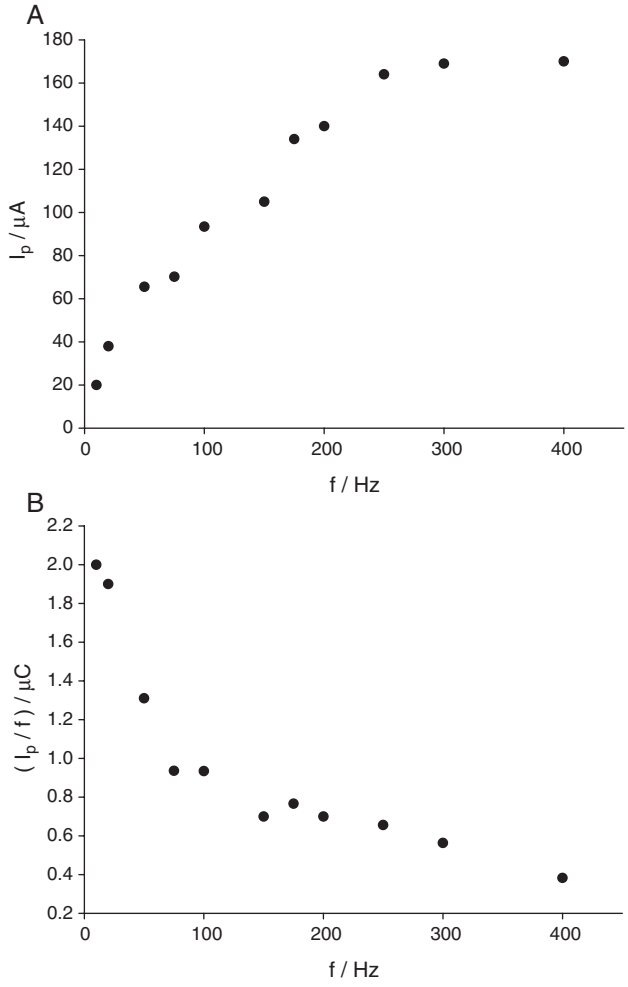

Fig. 6. Dependence of the net peak current (A) and the ratio between the net peak current and frequency (B) on the square-wave frequency. The response of the second redox center of adriamycin adsorbed on PIGE. Experimental conditions are as in Fig. 2.

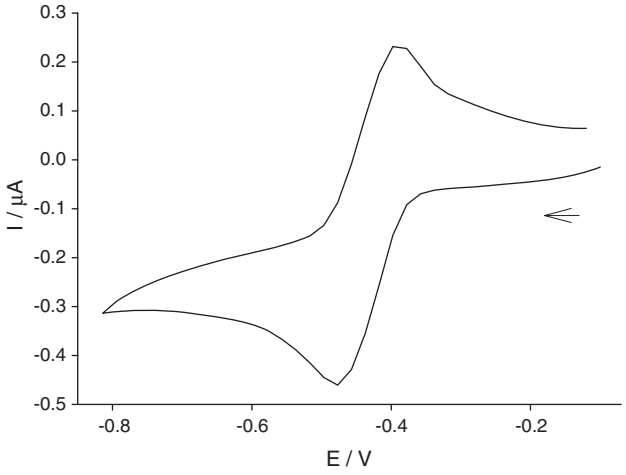

Fig. 7. Staircase cyclic voltammogram of adriamycin adsorbed on the surface of mercury electrode. The concentration of adriamycin is 1.72×10^{-4} mol/L and the supporting electrolyte is 0.9 mol/L KNO_3, pH 4.65. Adriamycin is accumulated during 30 s from unstirred solution, at −0.1 V. The scan rate is 0.1 V/s.

Fig. 3A shows the dependence of the net peak current of the first electrode process ($A+2e^-+2H^+\leftrightarrow C$, see Scheme 2) on the square-wave frequency. The dependence is sigmoidal up to 600 Hz, and decreases at higher frequencies due to the influence of capacitive currents [31]. Fig. 3B shows the ratio of the net peak current and the corresponding frequency plotted as the function of the frequency. This relationship exhibits the maximum for $f_{max}=100$ Hz. It was demonstrated previously [33] that the frequency f_{max} can be used for the calculation of the standard surface redox reaction rate constant using equation: $k_s=\kappa_{max} f_{max}$, where κ_{max} is the theoretically calculated critical kinetic parameter which depends on the number of electrons exchanged in the surface electrode reaction and on the square-wave amplitude. If the electron transfer coefficient α is not known exactly, an average kinetic parameter $\overline{\kappa}_{max}$, which applies to $0.2\le\alpha\le0.8$, can be used. For $n=2$ and $E_{sw}=50$ mV, $\overline{\kappa}_{max}=0.49\pm0.12$ [33]. So, the standard rate constant of the first electrode process is: $k_{s1}=49\pm12\ s^{-1}$.

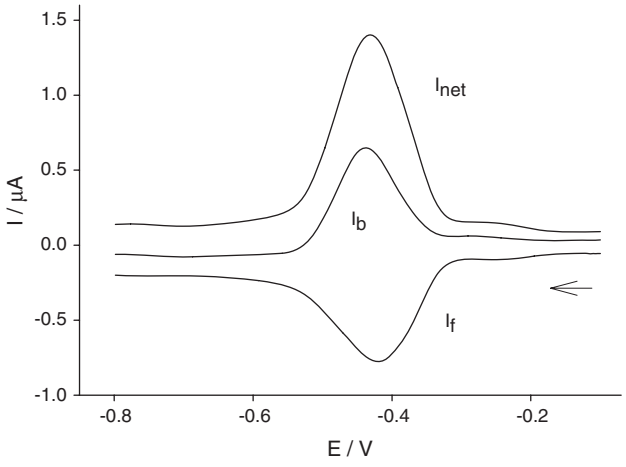

Fig. 8. Square-wave voltammetry of adriamycin adsorbed on mercury electrode. A net response and its forward and backward components. $E_{sw}=50$ mV, $f=10$ Hz and $dE=-2$ mV. All other experimental conditions are as in Fig. 7.

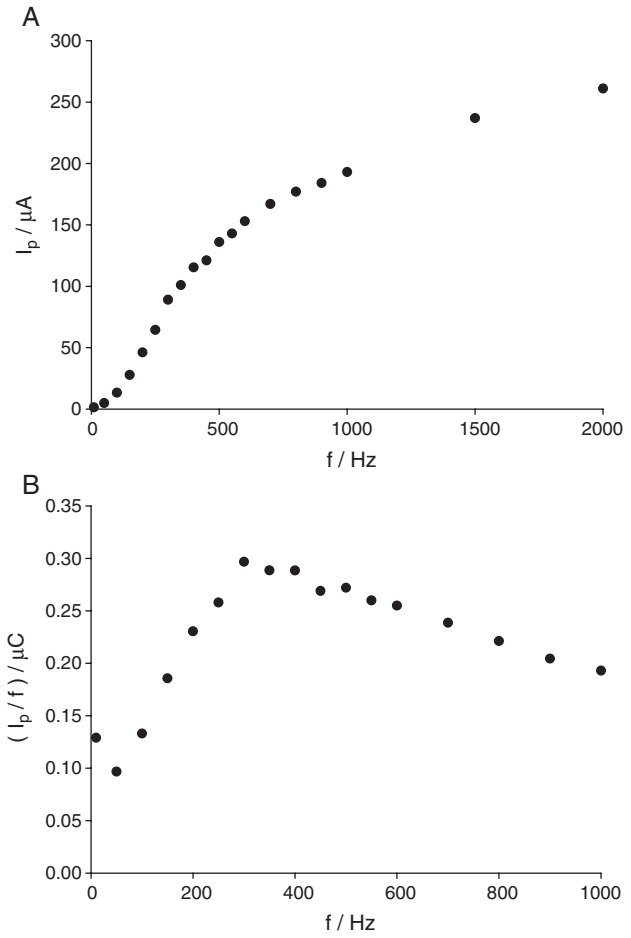

Fig. 9. Dependence of the net peak current (A) and the ratio between the net peak current and frequency (B) on the square-wave frequency. Experimental conditions are as in Fig. 8.

Fig. 4 shows that the response of the second redox couple depends on the starting potential. If the scan starts at +0.7 V, the peak potential of the net response is +0.30 V (Fig. 4A), but if it starts at 0 V, the net peak potential is +0.37 V (Fig. 4B). This is because the backward components of both responses are small, and the net responses depend on their forward components, mainly. In the first case the net response depends on the kinetics of the reduction of quinone moiety, while in the second one it depends on the kinetics of the oxidation of hydroquinone group. Fig. 5 shows the dependence of the net peak potential on the logarithm of the square-wave frequency, for the starting potential +0.7 V. This relationship can be approximated by a straight line, with a slope −0.083 V, which indicates that the electron transfer coefficient of the reduction of quinone group, marked by 2. in Scheme 2, is $\alpha_2 = 0.35$ [34]. If the starting potential is 0 V, the relationship between the net peak potential and the logarithm of frequency is approximately linear, with slope 0.045 V, which means that the transfer coefficient of the oxidation of hydroquinone is $\beta_2 = 0.65$ (not shown).

The relationship between the net peak current of the second electrode process and the square-wave frequency is shown in Fig. 6A and the dependence of the ratio of the net peak current and the frequency on the frequency is shown in Fig. 6B. The ratio I_p/f continuously decreases with the increasing frequency. Considering that $\alpha_2 = 0.35$, this means that $k_{s2} < 4\ s^{-1}$ [33].

Fig. 7 shows a cyclic voltammogram of adriamycin adsorbed on the surface of mercury electrode. The medium potential is −0.44 V and the peak separation is 80 mV. Adriamycin was accumulated from unstirred solution during 30 s at −0.1 V. Under the same conditions, the peak potential of the net response in square-wave voltammetry is −0.43 V, as can be seen in Fig. 8. The dependence of the net peak current and the ratio of the net peak current and frequency on the frequency is shown in Fig. 9. The latter relationship is in maximum for $f_{max} = 300$ Hz. So, the standard rate constant of the first redox couple on mercury electrode is $k_{s1} = 147 \pm 36\ s^{-1}$.

These experiments demonstrate that for the determination of the standard surface redox reaction rate constant the square-wave voltammetric net peak current–frequency relationship can be as useful as linear potential sweep voltammetry [35–38]. Electroanalytical methods for the determination of trace amounts of adriamycin are based on its adsorptive accumulation on carbon paste, or glassy carbon electrodes and on the detection of the response of electrooxidation of hydroquinone moiety in differential pulse voltammetry [22,23]. The present results show that on PIGE the reduction of quinone group of the adsorbed adriamycin is much faster that the oxidation of hydroquinone group. In square-wave voltammetry the highest response of the first group is achieved in the frequency range between 400 and 600 Hz, while the response of the second group is the highest at the frequency of 300 Hz. However, the optimum response of the first group is four times higher than the optimum response of the second group. So, the first one should be used for the electroanalytical determination of adriamycin. The results also indicate that the reduction of quinone is faster if adriamycin is adsorbed on mercury electrode than if it is adsorbed on PIGE. Probably, this is because the reduction on mercury occurs at 250 mV higher potential than on PIGE, which could mean that the adsorption of adriamycin is weaker on mercury than on PIGE. In square-wave voltammetry on mercury the optimum response is obtained at frequencies higher than 1000 Hz, but the adsorptive accumulation in situ is less effective than the procedure applied to PIGE.

Acknowledgement

A valuable gift from Dr. Mladen Ćepulić is gratefully acknowledged.

References

[1] F. Arcamone, Doxorubicin, Academic Press, New York, 1981, p. 354.
[2] J.W. Lown, Discovery and development of anthracycline antitumor antibiotics, Chem. Soc. Rev. 22 (1993) 165–176.
[3] G. Aubel-Sadron, D. Londos-Gagliardi, Daunorubicin and doxorubicin, anthracycline antibiotics, a physicochemical and biological review, Biochimie 66 (1984) 333–352.
[4] L. Türker, Quantum chemical studies on certain anthracycline antibiotics, J. Mol. Struc. (Theocem) 583 (2002) 81–87.

[5] A. Di Marco, F. Arcamone, F. Zunino, Anthracycline antibiotics, in: J. W. Corcoran, F.E. Hahn (Eds.), Antibiotics III—Mechanism of Action of Antimicrobial and Antitumor Agents, Springer, New York, 1975, pp. 101–128.
[6] M. Signorelli, A.A. Lissoni, A. Garbi, P. Perego, C. Mangioni, Primary malignant vaginal melanoma treated with adriamycin and ifosfamide: a case report and literature review, Gynecol. Oncol. 97 (2005) 700–703.
[7] R. Lin, L. Shi Ng, C.-H. Wang, In vitro study of anticancer drug doxorubicin in PLGA-based microparticles, Biomaterials 26 (2005) 4476–4485.
[8] J.L. Quiles, J.R. Huertas, M. Battino, J. Mataix, M.C. Ramirez-Tortosa, Antioxidant nutrients and adriamycin toxicity, Toxicology 180 (2002) 79–95.
[9] E.L. De Beer, A.E. Bottone, E.E. Voest, Doxorubicin and mechanical performance of cardiac trabeculae after acute and chronic treatment: a review, Eur. J. Pharmacol. 415 (2001) 1–11.
[10] J.R. Sporn, B.R. Greenberg, Empiric chemotherapy in patients with carcinoma of unknown primary site, Am. J. Med. 88 (1990) 49–55.
[11] C.A. Frederick, L.D. Williams, G. Ughetto, G.A. Van der Marel, J.H. Van Boom, A. Rich, A.H.J. Wang, Structural comparison of anticancer drug–DNA complexes: adriamycin and daunomycin, Biochemistry 29 (1990) 2538–2549.
[12] L.A. Lipscomb, M.E. Peek, F.X. Zhou, J.A. Bertrand, D. VanDarveer, L.D. Williams, Water ring structure at DNA interfaces: hydration and dynamics of DNA–anthracycline complexes, Biochemistry 33 (1994) 3649–3659.
[13] D.A. Gewirtz, A critical evaluation of the mechanism of action proposed for the antitumor effects of the anthracycline antibiotics adriamycin and daunorubicin, Biochem. Pharmacol. 57 (1999) 727–741.
[14] J. Wang, M. Ozsoz, X. Cai, G. Rivas, H. Shiraishi, D.H. Grant, M. Chicharro, J. Fernandes, E. Palaček, Interactions of antitumor drug daunomycin with DNA in solution and at the surface, Bioelectrochem. Bioenerg. 45 (1998) 33–40.
[15] M. Diociaiuti, A. Molinari, A. Calcabrini, G. Arancia, G. Isacchi, F. Bordi, C. Cametti, Alteration of the passive electrical properties of adriamycin-treated red cell membrane deduced from dielectric spectroscopy, Bioelectrochem. Bioenerg. 26 (1991) 177–192.
[16] H. Berg, G. Horn, U. Luthardt, W. Ihn, Interaction of anthracycline antibiotics with biopolymers: Part V. Polarographic behaviour and complexes with DNA, Bioelectrochem. Bioenerg. 8 (1981) 537–553.
[17] T. Konse, K. Kano, T. Kubota, Electrocatalytic reduction of oxygen at a pyrolytic graphite electrode modified by adriamycin and its 7-deoxyaglycone, J. Electroanal. Chem. 246 (1988) 385–397.
[18] A.M. Oliveira-Brett, M. Vivan, I.R. Fernandes, J.A.P. Piedade, Electrochemical detection of in situ adriamycin oxidative damage to DNA, Talanta 56 (2002) 959–970.
[19] J.A.P. Piedade, I.R. Fernandes, A.M. Oliveira-Brett, Electrochemical sensing of DNA–adriamycin interactions, Bioelectrochemistry 56 (2002) 81–83.
[20] G.M. Rao, J.W. Lown, J.A. Plambeck, Electrochemical studies of antitumor antibiotics, J. Electrochem. Soc. 125 (1978) 534–539.
[21] R.P. Baldwin, D. Packett, T.M. Woodcock, Electrochemical behavior of adriamycin at carbon paste electrodes, Anal. Chem. 53 (1981) 540–542.
[22] E.N. Chaney Jr., R.P. Baldwin, Electrochemical determination of adriamycin compounds in urine by preconcentration at carbon paste electrodes, Anal. Chem. 54 (1982) 2556–2560.
[23] A.M. Oliveira-Brett, J.A.P. Piedade, A.M. Chiorcea, Anodic voltammetry and AFM imaging of picomoles of adriamycin adsorbed onto carbon surfaces, J. Electroanal. Chem. 538–539 (2002) 267–276.
[24] S. Çakir, E. Biçer, E. Coşkun, O. Çakir, Electrochemical monitoring of the interactions of doxorubicin with nicotinamide and Fe(III) ions under aerobic and anaerobic conditions, Bioelectrochemistry 60 (2003) 11–19.
[25] E.N. Chaney, R.P. Baldwin, Voltammetric determination of doxorubicin in urine by adsorptive preconcentration and flow injection analysis, Anal. Chim. Acta 176 (1985) 105–112.
[26] J. Wang, M. Shan Lin, V. Villa, Adsorptive stripping voltammetric determination of low levels of daunorubicin, Analyst 112 (1987) 1303–1307.
[27] C. Yi, M. Gratzl, Continuous in situ electrochemical monitoring of doxorubicin efflux from sensitive and drug-resistant cancer cells, Biophys. J. 75 (1998) 2255–2261.
[28] J. Hu, Q. Li, Voltammetric behaviour of adriamycin and its determination at Ni ion-implanted electrode, Anal. Sci. 15 (1999) 1215–1218.
[29] D.E. Woolley, L.C. Tetlow, D.J. Adlam, D. Gearey, R.D. Eden, T.H. Ward, T.D. Allen, Electrochemical monitoring of anticancer compounds on the human ovarian carcinoma cell line A2780 and its adriamycin- and cisplatin-resistant variants, Exp. Cell Res. 273 (2002) 65–72.
[30] S. Zhang, K. Wu, S. Hu, Carbon paste electrode based on surface activation for trace adriamycin determination by a preconcentration and voltammetric method, Anal. Sci. 18 (2002) 1089–1092.
[31] Š. Komorsky-Lovrić, M. Lovrić, Measurements of redox kinetics of adsorbed azobenzene by a quasireversible maximum in square-wave voltammetry, Electrochim. Acta 40 (1995) 1781–1784.
[32] Š. Komorsky-Lovrić, Kinetics of the alizarine red S surface redox reaction, Fresenius' J. Anal. Chem. 356 (1996) 306–309.
[33] Š. Komorsky-Lovrić, Kinetics of the cinnoline surface redox reaction, Electroanalysis 14 (2002) 888–891.
[34] M. Lovrić, Square-wave voltammetry, in: F. Scholz (Ed.), Electroanalytical Methods, Springer, Berlin, 2002, pp. 111–136.
[35] E. Laviron, General expression of the linear potential sweep voltammogram in the case of diffusionless electrochemical system, J. Electroanal. Chem. 101 (1979) 19–28.
[36] E. Laviron, Y. Mugnier, A study of the surface and volume electroreduction of *cis*- and *trans*-azobenzene in protic media, J. Electroanal. Chem. 111 (1980) 337–344.
[37] M. Mladenov, V. Mirčeski, I. Gjorgoski, B. Jordanoski, Redox kinetic measurements of glutathione at the mercury electrode by means of square-wave voltammetry. The role of copper, cadmium and zinc ions, Bioelectrochemistry 65 (2004) 69–76.
[38] Y. Wu, X. Ji, S. Hu, Studies of electrochemical oxidation of azithromycin and its interaction with bovine serum albumin, Bioelectrochemistry 64 (2004) 91–97.